

SOCS1-KIR Peptide in PEGDA Hydrogels Reduces Pro-Inflammatory Macrophage Activation

Aakanksha Jha, Joseph Larkin III, and Erika Moore*

Macrophages modulate the wound healing cascade by adopting different phenotypes such as pro-inflammatory (M1) or pro-wound healing (M2). To reduce M1 activation, the JAK/STAT pathway can be targeted by using suppressors of cytokine signaling (SOCS1) proteins. Recently a peptide mimicking the kinase inhibitory region (KIR) of SOCS1 has been utilized to manipulate the adaptive immune response. However, the utilization of SOCS1-KIR to reduce pro-inflammatory phenotype in macrophages is yet to be investigated in a biomaterial formulation. This study introduces a PEGDA hydrogel platform to investigate SOCS1-KIR as a macrophage phenotype manipulating peptide. Immunocytochemistry, cytokine secretion assays, and gene expression analysis for pro-inflammatory macrophage markers in 2D and 3D experiments demonstrate a reduction in M1 activation due to SOCS1-KIR treatment. The retention of SOCS1-KIR in the hydrogel through release assays and diffusion tests is demonstrated. The swelling ratio of the hydrogel also remains unaffected with the entrapment of SOCS1-KIR. This study elucidates how SOCS1-KIR peptide in PEGDA hydrogels can be utilized as an effective therapeutic for macrophage manipulation.

1. Introduction

Wound healing is critical for the restoration of tissue functionality and integrity.^[1] An essential stage in wound healing is

inflammation, which defends the body against injurious stimuli such as damaged cells or pathogens. During inflammation, immune cells are recruited to the site of injury by spatiotemporal cues.^[2] Depending on the cues, cytokines direct the immune response during wound healing through propagation of inflammation or regeneration.^[3] If the immune response stalls in the stages of inflammation, a healthy wound can transition to a non-healing chronic wound.

Macrophage immune cells are recruited to wound beds or sites of injury to expunge foreign pathogens via phagocytosis.^[4] Once recruited, macrophages can exist on a spectrum exhibiting different phenotypes which are dictated by extracellular cues such as cytokines. Macrophages can adopt a pro-inflammatory (M1) or classically activated phenotype.^[5] Macrophages can also adopt an inflammation resolution phenotype called M2 or alternatively activated.^[5,6]

The phenotypes can exist concurrently in vivo, although for in vitro studies, we bin phenotypes as M1 or M2.^[7] The ratio of macrophages from M1 to M2 changes as wounds progress. For example, in a regular dermal wound 85% macrophages are of the M1 phenotype during inflammation while the number of M1 macrophages reduces to about 15% during regeneration.^[8] However, in chronic wounds, macrophages remain predominantly M1 (~80%),^[9] thereby preventing healing and regeneration of such chronic wounds. Exorbitant productions of inflammatory cytokines can lead to the over-population of M1 macrophages.^[10] By targeting pathways to reduce inflammatory cytokine expression, M1 macrophage activation can be reduced which could pave the way for therapeutic interventions in chronic wounds.

Activation of janus kinases (JAK), and signal transducers and activators of transcription (STAT) are involved in the production of inflammatory cytokines.^[11] The JAK/STAT pathway can be modulated by regulatory proteins that control the intensity and duration of cytokine responses.^[12,13] Suppressor of cytokine signaling (SOCS) proteins are negative feedback regulators that directly interact with JAKs by binding to the cytokine receptor or JAK. The bind between a segment of SOCS and cytokine receptor/JAK creates an obstruction by inhibiting phosphorylation, which prevents recruitment and activation of STATs to the signaling cascade, thereby inhibiting translocation of the inflammatory signal to the cell.^[14] SOCS1, one of the 8 members of the SOCS family, has been shown to play a key role in the molecular

A. Jha


J. Crayton Pruitt Family Department of Biomedical Engineering
Herbert Wertheim College of Engineering
University of Florida
Gainesville, FL 32611, USA

J. Larkin III

Department of Microbiology and Cell Science
University of Florida
Gainesville, FL 32603, USA

E. Moore

Fischell Department of Bioengineering, A. James Clark School of Engineering
University of Maryland
College Park, MD 20742, USA
E-mail: emt@umd.edu

 The ORCID identification number(s) for the author(s) of this article can be found under <https://doi.org/10.1002/mabi.202300237>

© 2023 The Authors. Macromolecular Bioscience published by Wiley-VCH GmbH. This is an open access article under the terms of the Creative Commons Attribution-NonCommercial-NoDerivs License, which permits use and distribution in any medium, provided the original work is properly cited, the use is non-commercial and no modifications or adaptations are made.

DOI: 10.1002/mabi.202300237

recognition of cytokine signaling.^[15,16] SOCS1 regulates immune homeostasis and has been shown to prevent inflammation. SOCS1 can promote degradation of intracellular proteins that are imperative to propagate cytokine-mediated inflammatory cascades. Previous studies have utilized the SOCS1 protein to understand its role in the regulation of activation states of murine monocyte-derived macrophages.^[17,18] Downregulation of SOCS1 expression was shown to upregulate the JAK/STAT pathway and alter macrophage activation by promoting pro-inflammatory macrophages. Although changes in SOCS1 expression were conducive to manipulating macrophage polarization, there has been no clear understanding of its mechanism. SOCS1 protects the host from the lethal lipopolysaccharide (LPS) response and this has been verified in a model of SOCS1-deficient mice.^[19]

The kinase inhibitory region (KIR) possessed by SOCS1 inhibits kinase activity of JAK members, particularly JAK2.^[20,21] Among other regions of the SOCS protein chain, the KIR region was preferentially isolated after studies suggested its direct role in inflammatory disease modulation. Recent studies have utilized a peptide mimic of the KIR region of SOCS1 to ameliorate inflammatory diseases such as multiple sclerosis and systemic lupus erythematosus.^[22,23] The SOCS1-KIR peptide mimics active ligands of cytokines and other biomolecules and was initially designed complementarily to the JAK2 activation loop.^[20] SOCS1-KIR mimetics have successfully inhibited inflammatory cytokine signaling by targeting the JAK/STAT pathway in two-dimensional (2D) environments.^[24,25] An advantage of using SOCS1-KIR peptide mimetics over whole SOCS1 proteins is that these mimetics can easily be absorbed by the body, and readily cross the blood brain barrier due to their smaller structure.^[14] SOCS1-KIR peptides are being considered in the clinic.^[14] A useful and unexplored tool for the utilization of SOCS1-KIR peptide would be in a three-dimensional (3D) hydrogel environment. The entrapment of SOCS1-KIR to validate it as a macrophage manipulator in a 3D system is novel to this work. Sequestering the JAK/STAT pathway by using SOCS1-KIR peptide to manipulate the innate and adaptive immune response is beneficial to exploring treatments for chronic inflammatory diseases.

In this work, we aim to reduce pro-inflammatory M1 macrophage activation by utilizing a SOCS1-KIR peptide dimer entrapped within a poly(ethylene glycol) diacrylate (PEGDA) hydrogel. To our knowledge, no prior work has incorporated SOCS1-KIR peptide in a PEG-based hydrogel for local inhibition of inflammatory macrophages. We hypothesize that SOCS1-KIR in a PEGDA hydrogel will reduce activation of pro-inflammatory (M1) macrophages. SOCS1-KIR can be used as a soluble treatment for M1 inhibition or while being entrapped amidst the meshes of the branched polymer network of PEGDA and PEG-Arg-Gly-Asp-Ser (RGDS).^[26] Soluble treatment of SOCS1-KIR on murine and human macrophages displays a robust reduction in pro-inflammatory markers via gene expression and immunocytochemistry. In the hydrogel we graft RGDS, a fibronectin derived peptide for cell adhesion.^[27,28,29] The hydrogel is evaluated for its efficiency in entrapping the SOCS1-KIR peptide via structural and mechanical characterization assays. The characterization assays prove that SOCS1-KIR is being retained in the hydrogel, which is beneficial for the macrophages encapsulated within the hydrogel. Our work demonstrates that the use of SOCS1-KIR in a PEGDA hydrogel reduces M1 macrophage activation via im-

munocytochemistry, gene expression analyses, and soluble protein quantification. These results display a functional hydrogel design that can be used to modulate macrophage function. Utilizing this design enables harnessing the properties of SOCS1-KIR to reduce M1 macrophage activation in murine and human macrophages.

2. Experimental Section

2.1. Cell Culture and Maintenance

Raw 264.7 macrophages (ATCC) were cultured in Dulbecco's Modified Eagle's Medium (DMEM) (Corning, Corning, NY) supplemented with 10% fetal bovine serum (FBS) (Atlanta Biologicals, Lawrenceville, GA), 100 IU penicillin, and 100 µg mL⁻¹ streptomycin (Corning). For the purposes of this article, this was labeled M0 media. Macrophages in the presence of M0 media were referred to as M0 macrophages. To stimulate the macrophages toward the M1 phenotype, 10 ng mL⁻¹ of interferon gamma (IFNγ) (Prospec, East Brunswick, NJ) along with 100 ng mL⁻¹ of lipopolysaccharide (LPS) (Santa Cruz Biotechnology, Dallas, TX) was added to M0 media. This is referred to as M1 media. Macrophages stimulated by M1 media were referred to as M1. Macrophages were stimulated to the M1 phenotype 24 h post-seeding on a 24-well tissue culture polystyrene (TCP) plate and 2 h post-peptide treatment. M0 macrophages were also cultured over the same time periods, resulting in two groups across 24, 48, and 72 h (M0 and M1 with and without SOCS1-KIR peptide). All macrophages were maintained at 37 °C in 5% CO₂.

Human peripheral blood derived monocytes (PBMcs) from a healthy 30-year-old Caucasian female were purchased from Hemacare, Charles River Laboratory (#IRB202101975). Cryopreserved monocytes allowed the production of more homogeneous macrophage cultures while also reducing dependency on donor variability. The monocytes were thawed in Hanks' Balanced Salt Solution (HBSS) without calcium or magnesium, 10% heat inactivated human (AB) serum (Millipore Sigma, Burlington, MA), and Roswell Park Memorial Institute (RPMI) 1640 (Fisher Scientific, Hampton, NH) (according to manufacturer's protocol). The culture media for differentiating monocytes to macrophages consisted of RPMI 1640, 10% heat inactivated human (AB) serum, 100 IU penicillin, and 100 µg mL⁻¹ streptomycin. Macrophage colony-stimulating factor (M-CSF) (20 ng mL⁻¹) was added for the differentiation of monocytes to macrophages. Cells were plated at a density of 0.1 × 10⁶ cells mL⁻¹ in two tissue culture (TC) treated 24-well plates for 2D experiments and one 12-well plate for 3D experiments. Monocytes were incubated at 37 °C with 5% CO₂ for 5 days with a media change on day 3. In the presence of M-CSF, monocyte derived macrophages were polarized to the M1 phenotype on day 5. The M1 or classically activated macrophages were stimulated with 100 ng mL⁻¹ of LPS and 10 ng mL⁻¹ of IFNγ with the culture media. For stimulation to the M2 phenotype, 20 ng mL⁻¹ of interleukin (IL)-4 (Prospec, East Brunswick, NJ) was added the media and these macrophages were referred to as M2. Macrophages were stimulated for 2 days in 37 °C with 5% CO₂ and processed for further data generation on day 7. All macrophages were either lysed in the wells to obtain RNA or fixed with 4% paraformaldehyde for immunostaining. The supernatant was collected to perform a human cytokine

array ELISA. Macrophages were gently scraped to lift them off the plates for encapsulations or rinsing steps.

2.2. 2D Experiments of SOCS1-KIR

For 2D experiments in murine macrophages, cells were plated on top of glass coverslips in 24-well plates at 0.1×10^6 cells mL⁻¹. After seeding, macrophages were allowed to adhere overnight in 37 °C with 5% CO₂. Cells were pre-treated with 33 μM SOCS1-KIR peptide for 2 h to allow penetration of the peptide into cells and left in the incubator. After peptide treatment, the macrophages were stimulated to the M1 phenotype as discussed in prior sections. M0 and M1 macrophages with and without SOCS1-KIR treatment were processed at 24, 48, and 72 h for further analysis.

The 2D experiments for human macrophages followed the same method as for murine macrophages. Samples were only processed at 48 h post M1 stimulation and peptide treatment. The timepoint of 48 h was selected because of previous studies demonstrating successful inhibition of pro-inflammatory mediators with 48 h SOCS1-KIR treatment.^[24] Supernatant was collected to assess pro-inflammatory cytokines through a human cytokine array enzyme linked immunosorbent assay (ELISA).

2.3. Fabrication of PEGDA-SOCS Hydrogels

PEGDA (MW = 10 kDa) was obtained from Laysan Bio Inc., Arab, AL (#20861). The cell-adhesive component RGDS (MW = 433.42 Da) was conjugated to acrylate-poly (ethylene glycol) (PEG)-succinimidyl valerate (SVA) (MW = 3400 Da) (Laysan Bio Inc., Arab, AL) to obtain acryl-PEG-RGDS (MW = 3833.42 Da) via amine substitution chemistry. The crosslinking chemistry has been previously described.^[23–24,27,28,30–32] The hydrophobic acryl groups self-assembled to form micelle-like centers in the presence of (*N*-(2-Hydroxyethyl) piperazine-*N'*-(4-butanedisulfonic acid)) (HEPES) buffer. With constant agitation and titrations (pH = 8) by adding 0.1 M NaOH, a covalently linked PEG-peptide reaction was obtained. Dialysis occurred over night with a 3.5 kDa MWCO cellulose membrane (Spectrum Laboratories) for purification of PEG-RGDS. The SOCS1-KIR peptide (MW = 4752 Da) was obtained from our collaborator (J.L. III)^[22,23] in the department of Microbiology and Cell Science at the University of Florida. The SOCS1-KIR peptide was generated by the Larkin group using Applied Biosystems 431a automated peptide synthesizer (Applied Biosystems, Carlsbad, CA) by conventional fluorenylmethylcarbonyl chemical methods. A palmitoyl-lysine (a lipophilic group) was added to the N-terminus of the peptides during the final step to assist in cell penetration.^[22] A working concentration of 33 μM was determined to be biologically relevant for cell instruction as previously defined.^[24] SOCS1-KIR dimer sequence is ⁵³DTHFRTRSHSDYRRI, where 53 represents the beginning of the amino acid sequence for the KIR region on the endogenous SOCS1 protein.

The “control” hydrogel (PEGDA+PEG-RGDS) was formed with 10% PEGDA, 3.5 mM PEG-RGDS, 10 μM eosin Y, and 0.35% *N*-vinyl pyrrolidone (NVP) in HEPES and 1.5% triethanolamine (TEOA). Using the control hydrogel design as the foundation,

33 μM SOCS1-KIR was added to the polymer solution to obtain the “experimental” or PEGDA-SOCS hydrogel. Therefore, the PEGDA-SOCS hydrogel or in short PEG-SOCS was formed with 10% PEGDA, 3.5 mM PEG-RGDS, 10 μM eosin Y, 0.35% NVP, and 33 μM SOCS1-KIR. In the experimental PEG-SOCS hydrogel, SOCS1-KIR peptide was not covalently conjugated to PEG but rather interspersed in a network of PEG-RGDS and PEGDA, the entirety of which was crosslinked into a hydrogel. A 5 μL volume of macrophages and polymer solution was pipetted onto PDMS slabs with two 385 μm thick PDMS spacers. The droplet was exposed to white light for 60 s underneath a methacrylated cover slip which allowed for attachment of the PEG hydrogel to the coverslip. White light exposure activated eosin Y (photoinitiator) which led to free radical generation allowing crosslinking and thus, rapid polymerization of the hydrogel. The hydrogel was then placed in 24-well plates and macrophage media was gently pipetted in the wells.

2.4. 3D Experiments of SOCS1-KIR

All 3D experiments with murine macrophages encapsulated in control or PEG-SOCS (or SOCS) hydrogels continued for 5 days and 10 days post encapsulation. Macrophages were encapsulated in control and SOCS hydrogels at 1×10^7 cells mL⁻¹ (≈50 000 cells per gel). Encapsulation was performed on day 1 in both hydrogel groups. M1 stimulation occurred 24 h later (day 2) to allow macrophage acclimatization in the hydrogel. The M1 stimulated and unstimulated macrophages in gels were fixed 72 h (day 5) post-M1 stimulation for further analyses. The 10-day experiment followed the same timeline but with M0 media for all groups after day 5. The macrophages were then fixed on day 10 for immunostaining.

The 3D experiments for human macrophages were performed in a similar manner to murine macrophages, i.e., for 5 days with the timeline described above. Supernatant was collected for further analysis or aspirated.

2.5. Immunofluorescence Staining

For immunofluorescence staining, both murine and human macrophages in 2D and 3D cultures were fixed with 4% paraformaldehyde for 25 min (2D) or 45 min (3D) followed by rinses with tris-buffered saline (TBS) at room temperature (RT). Permeabilization of the cell membrane occurred by treating with 0.125% Triton-X for 10 min (2D) or 0.25% Triton-X for 45 min (3D) at RT, followed by TBS rinses. Samples were then blocked with 5% donkey serum (DS) for 3 h (2D) or overnight (3D) at 4 °C, followed by TBS rinses. Then, 2D and 3D samples were incubated overnight with primary antibody iNOS (Rabbit Anti-Mouse Polyclonal Antibody, Invitrogen, Waltham, MA) at 1:400 dilution with 0.5% DS. In addition to iNOS, for the human macrophage samples in 2D, the primary antibody used was CD206 (Goat Anti-Mouse Polyclonal Antibody, Invitrogen, Waltham, MA; 1:400). The samples were rinsed 6 times for 20 min (2D) or 90–120 min (3D) each; the first five rinses were with 0.01% Tween diluted in TBS, and the last rinse was TBS only. The samples were then incubated with secondary antibody-Alexa Fluor 555 Donkey Anti-Rabbit for iNOS (1:200; Thermo Fisher Scientific, Waltham, MA),

Table 1. Primer sequences for genes used in RT-PCR experiment.

RpLp0	Forward	AGATTCGGGATATGCTGTTGGC
	Reverse	TCCGGTCCTAGACCAAGTTC
PpiA	Forward	GAGCTGTTGCAGACAAAGTTC
	Reverse	CCCTGGCACATGAATCCTGG
iNOS	Forward	TTTGCTTCCATGCTAATGCGAAAG
	Reverse	GCTCTGTTGAGGTCTAAGGCTCCG
TNF α	Forward	CCTGTAGCCCACTCGTAGC
	Reverse	AGCAATGACTCCAAAGTAGACC

and Alexa Fluor 488 Donkey Anti-Goat for CD206 (1:200; Thermo Fisher Scientific, Waltham, MA) overnight at 4 °C. Secondary staining was followed by an hour-long TBS rinse. Cell nuclei were stained with 2 μ M 4',6-diamidino-2-phenylindole (DAPI; Thermo Fisher Scientific, Waltham, MA) followed by two rinses with TBS for 5mins each.

2.6. Imaging and Image Analysis

The post-stimulation and polarization effects of SOCS1-KIR peptide inhibiting iNOS expression in M1 macrophages were evaluated by imaging on the Keyence BZ-X800 microscope. Images were quantified based on the number of cells that showed a positive stain for iNOS (iNOS⁺), normalized to the total cell count as confirmed by a positive stain for DAPI (DAPI⁺). For 2D experiments, five images were taken per well. For 3D hydrogel experiments, five images were taken per hydrogel and the images were captured as single frames across various areas in the hydrogel. The overlay of iNOS and DAPI images were imported into ImageJ. The image was split into its respective channels using the “Color>Split channels” function. The split channels function automatically converts the DAPI (blue) and iNOS (red) channels into 8-bit grayscale monochrome images. Images were thresholded and cells were counted using ImageJ’s “automated cell counting of single color image” feature. The normalized counts of iNOS⁺/DAPI⁺ cells were exported to GraphPad Prism for further statistical analyses. The representative immunofluorescent images were overlays of DAPI (blue) and iNOS (red) stained macrophages. Same steps were followed for CD206⁺/DAPI⁺ expression analysis when needed.

2.7. Enzyme-Linked Immunosorbent Assay (ELISA)

Human monocyte derived macrophages, pre-treated with 33 μ M SOCS1-KIR peptide and stimulated to M1, were assessed for pro-inflammatory cytokine secretion. The conditioned media or cell supernatant was collected at 48 h to assess differences in pro-inflammatory cytokine. Protocol was followed according to the manufacturer’s instructions as provided in the human cytokine array ELISA kit (Anogen, Yes Biotech Laboratories Ltd., Canada). The cytokines assessed were IFN γ , tumor necrosis factor alpha (TNF α), monocyte chemotactic and activating factor (MCAF), and granulocyte macrophage colony stimulating factor (GM-CSF). The concentrations of listed cytokines were measured

at 450 nm using a BioTek Synergy HT Plate reader. Histogram plots for observing trends were created by comparing the concentrations of each cytokine for M1 versus M1+SOCS.

2.8. Reverse Transcription-Polymerase Chain Reaction (RT-PCR)

Total RNA was isolated using a TRIzol (Invitrogen) extraction method and quantified using NanoDrop spectrophotometer (Thermo Scientific). Reverse transcription was performed with 1 μ g of total RNA using the iScript cDNA Synthesis Kit (BioRAD). Complementary DNA was amplified using the SYBR Green PCR Master Mix (BioRAD). The primer sequences (IDT) used for PCR analysis are listed in Table 1. The cycling parameters were as follows: 95 °C for 15 s, 60 °C for 30 s, and then 72 °C for 30 s for a total of 40 cycles. The expressions of iNOS and TNF α mRNA were normalized to Ribosomal Protein Large P0 (RpLp0) and Peptidyl-prolyl Isomerase A (PpiA) with the M1 groups used as a control. Both endogenous reference genes RpLp0 and PpiA had comparable standard deviations, thus RpLp0 was chosen as the housekeeper gene for all analyses. Expression levels of genes of interest were calculated using the comparative delta–delta cycle threshold (C_T) method.

The delta–delta Ct method, also known as the 2^{− $\Delta\Delta$ Ct} method, was used to calculate the relative fold gene expression of samples when performing RT-PCR.

2.9. NanoString Gene Expression Analysis

RNA was lysed directly in the wells and isolated by adding to the Qiagen RNeasy Plus Micro Kit (following the manufacturer’s protocol). The isolated RNA was stored at −80 °C until use. The quality and concentration of RNA was accepted between 1.9 and 2.1 (260/280) as quantified by a BioTek Synergy HT plate reader. RNA was diluted to a concentration of 5 ng μ L^{−1} for a total input of 25 ng per sample as recommended by the Nanostring protocol. The nCounter Myeloid Innate Immunity V2 Panel was utilized for gene expression analysis of samples. Diluted RNA (25 ng input, 5 μ L volume) was added to a combination of reporter probe set (8 μ L diluted with hybridization buffer) and capture set (2 μ L) reagent per sample. The 15 μ L total mixture of probes and samples were hybridized for 16–20 h at 65 °C with the lid of thermal cycler at 70 °C. Post hybridization, the samples were brought up to a total volume of 30 μ L by adding hybridization buffer. The nSolver 4.0 software kit was utilized for

data processing. The Myeloid Innate Immunity V2 panel has 770 genes including 40 internal reference genes—housekeepers; positive controls (spiked in during manufacturing codesets); negative controls (not spiked in, no targets present for these probes) for data normalization. Pathways were analyzed from the annotated gene set global significance score, calculated as the square root of the mean squared *t*-statistics of genes. These data are used to evaluate the gene expression profile of human monocyte derived macrophages polarized to different phenotypes and treated with the SOCS1-KIR peptide to reduce pro-inflammatory (M1) activation. Heatmaps were created for genes related to M1 pro-inflammatory macrophages, SOCS or JAK/STAT pathway related genes as well as the genes encoded for cytokines assessed in the ELISA for pro-inflammatory cytokines. Heatmaps were generated by plotting log2 fold change values to highlight the gene expression differences between M0 and M1 macrophages with and without SOCS1-KIR treatment.

2.10. FITC-Dextran Experiment

To create hydrogels embedded with Fluorescein isothiocyanate-dextran (FITC-Dextran), (3–5 kDa) (Sigma Aldrich St. Louis, MO, USA), the “control” or PEGDA+PEG-RGDS hydrogels were loaded with 33 μM FITC-Dextran. The two hydrogel groups were “control” and “FITC-Dextran” ($n = 8$). Herein, FITC-Dextran acted as a surrogate for SOCS1-KIR peptide. The concentration of SOCS1-KIR at 33 μM was 0.156.8 $\mu\text{g mL}^{-1}$. Therefore, the same concentration of FITC-Dextran was loaded in the hydrogel. All gels were placed in 24-well plates immersed in 1 mL PBS, wrapped in foil, and incubated at 37 °C overnight. After 24 h of encapsulation, the PBS (supernatant) was replaced with fresh PBS. The supernatant was carefully placed in a 96-well plate with triplicates (from the same well) of 100 μL for quantification of mean fluorescence intensity (MFI). The FITC-Dextran experiment mimicked the 5-day encapsulation experiments wherein M1 stimulation occurred at 24 h, and samples were fixed at 72 h post-stimulation. For the FITC-Dextran experiment, complete replacement of diluent took place at 24 h with no further changes or dilutions until supernatant was collected at 72 h. Release of FITC-Dextran was assessed at 24 and 72 h by measuring MFI. As an additional control MFI of eosin Y/NVP and FITC-Dextran in solution was also measured. The FITC-Dextran content in samples was quantified using a BioTek Synergy HT plate reader at excitation and emission wavelengths of 490 and 520 nm, respectively.

2.11. Protein Release Assay

Release or retention of SOCS1-KIR protein was assessed by a bicinchoninic acid assay (BCA; Pierce BCA Protein Assay Kit #23227; Thermo Fisher Scientific, Waltham, MA). The hydrogel groups were PEGDA, PEGDA+PEG-RGDS (PEG-RGDS), and PEGDA+PEG-RGDS+SOCS1-KIR (PEG-SOCS) ($n = 3$ for each group). The hydrogels were incubated in 1 mL phosphate buffered saline (PBS) for 7 days. Supernatant PBS (500 μL) was collected and replaced with fresh 500 μL PBS every day until day 7 to generate a cumulative release curve. Retention was quantified iteratively with partial replacement of diluent every day. PBS

solution was used as a calibration standard. Collected PBS samples were frozen in $-20\text{ }^{\circ}\text{C}$ until BCA could be conducted. Following manufacturer’s instructions, the absorbance from the 96 well plate was read at 562 nm using a BioTek Synergy HT plate reader.

2.12. PEGDA-SOCS Hydrogel Swelling Experiment

For swelling studies, control and PEGDA-SOCS hydrogels ($n = 12$) were weighed immediately after polymerization to determine the initial weight (W_i). The hydrogels were then immersed in 1 mL PBS in 24-well plates and incubated at 37 °C for 24 h. Post-absorption, hydrogels were blotted to remove extra liquid and weighed for final swollen weight (W_s). Swelling ratio (SR) of the hydrogels was calculated according to Equation (1):

$$\text{Swelling ratio} = W_s - W_i / W_i \quad (1)$$

2.13. Statistical Analyses

Images were quantified as iNOS⁺ cells normalized to total cell count represented by DAPI⁺ cells. Imaging analysis was recorded in Microsoft excel, and then exported to GraphPad Prism for further quantification. To obtain statistical significance, one-way ANOVA with Tukey’s post hoc comparison tests were performed for all 2D and 3D experiments. A Student’s *t*-test was also performed to compare DAPI cell counts per view field between the M1 groups with and without SOCS1-KIR ($*p < 0.05$) across all time points. Cohen’s *d* value was used to quantify effect size of SOCS1-KIR in reducing iNOS⁺ cells over 24, 48, and 72 h. The means and pooled standard deviations of iNOS⁺ M1 macrophages were compared to SOCS1-KIR treated iNOS⁺ M1 macrophages. The swelling experiment and FITC-Dextran experiment were analyzed via Student’s *t*-test to evaluate statistical significance. The BCA assay was evaluated with a one-way ANOVA with Tukey’s multiple comparison tests. Nanostring gene expression data were evaluated by forming a volcano plot and heatmaps for better visualization. The volcano plot was generated by conducting a pathway analysis from the annotated gene set global significance score, calculated as the square root of the mean squared *t*-statistics of genes. Adjusted *p*-values were obtained from post-hoc corrections using Benjamini–Yekutieli method. The log2 fold change values were plotted against $-\log_{10}$ of the *p*-values. The volcano plot indicated trends and not statistical significance. Heatmaps were created by plotting the normalized log2 counts of M1 groups with and without SOCS1-KIR treatment.

3. Results and Discussion

Macrophages are highly plastic immune cells that can direct the immune response toward inflammation resolution or toward chronic inflammation.^[4,32] Engineering biomaterials that can guide macrophage function are beneficial therapeutics to direct wound healing. SOCS has been shown to be critical to lymphocyte activation and differentiation.^[33] Controlling inflammatory responses by targeting the JAK/STAT pathway using negative regulators such as proteins from the SOCS family is an

advantageous strategy for the manipulation of the innate immune response.^[14,20,33] For example, there are clinically approved JAK/STAT inhibitors like tofacitinib (JAK3 inhibitor) to treat conditions such as alopecia areata and rheumatoid arthritis.^[34] There is still much exploration due around SOCS1 mimicking peptides, thus in vitro models are a great platform to investigate and leverage its benefits toward modulating the innate immune system. Additionally, evaluating the effects of SOCS1-KIR peptide treatment on the genetic profile of macrophages is the first of its kind. In this work, we introduce a biomaterial utilizing PEGDA for entrapping SOCS1-KIR peptide to reduce activation of pro-inflammatory M1 macrophages.

3.1. SOCS1-KIR Peptide Reduces Pro-Inflammatory Markers in 2D Cultures of Murine Macrophages

To investigate the effects of SOCS1-KIR on macrophage activation, we first analyzed its effects in 2D by exposing murine Raw 264.7 macrophages to the peptide and subsequently stimulating the macrophages to different phenotypes. M0 or unstimulated macrophages were used as the control group. M1 macrophages were obtained by stimulating M0 macrophages using LPS, component of gram-negative bacterial wall, and IFN γ , a soluble pro-inflammatory cytokine. Macrophages were seeded on TCP and allowed to adhere overnight. Macrophage cultures were treated with palmitated SOCS1-KIR for 2 h to allow for plasma membrane penetration.^[35] A study by Jager et al. demonstrated SOCS1-KIR to be most effective in inhibiting pro-inflammatory cytokine response using splenocytes as well as Raw 264.7 macrophages at 33 μ M.^[24] To maintain the therapeutic efficacy of SOCS1-KIR and leverage it for inhibiting macrophage activation, the concentration of 33 μ M was deemed appropriate. Post-peptide treatment, macrophages were stimulated toward M1 for 24, 48, and 72 h (Figure 1a,b).

To quantify macrophage response, we utilized iNOS, an enzyme used as a canonical M1 macrophage marker. iNOS is released in abundance under oxidative stress or in response to cytokines, and contributes to killing pathogens.^[36] Particularly, inflammatory cells express iNOS when activated in the later phases of infection.^[36,37] An overexpression of iNOS in chronic wounds leads to impaired healing by preventing phenotypic switching of macrophages thus stagnating the inflammatory environment.^[38] Hence, it is important to reduce pro-inflammatory factors like cytokines and iNOS in the environment. Reduction in iNOS expression indicates reduced M1 activation. Macrophages were stained for DAPI (nucleus marker) and iNOS (M1 marker) and then quantified for iNOS⁺/DAPI⁺ cells or in other words iNOS expression per total DAPI positive cells. Ratios of differences between iNOS expression in M0 and M1 macrophages with and without SOCS1-KIR treatment are represented for 24, 48, and 72 h (Figure 1a). iNOS⁺/DAPI⁺ cell count of 1 implies that 100% of all the DAPI⁺ cells are positive for iNOS expression. M1 stimulated macrophages are expected to have a higher ratio of iNOS⁺/DAPI⁺ count. The difference between the M1 stimulated groups with and without SOCS1-KIR treatment was drastic. iNOS⁺ cells normalized to DAPI⁺ cells were 0.86 ± 0.09 in M1 compared to 0.14 ± 0.04 in the M1+SOCS group over 24 h (Figure 1a). A one-way ANOVA revealed that the pres-

ence of SOCS1-KIR significantly reduced iNOS expression in M1 macrophages. At the 24 h stimulation timepoint, we found that M0 macrophages had negligible iNOS expression with the M0 group at 0.04 ± 0.01 iNOS⁺/DAPI⁺ cells, and M0+SOCS at 0.02 ± 0.01 iNOS⁺/DAPI⁺ cells (Figure 1a). M0 macrophages with minimal iNOS positivity was expected as there was no stimulating factor present to induce iNOS expression. Therefore, at 24 h, SOCS1-KIR successfully reduced iNOS expression demonstrating inhibition of pro-inflammatory M1 activation.

Similarly, at 48 h, iNOS⁺ macrophages were significantly reduced in the M1+SOCS group. iNOS⁺/DAPI⁺ cell count reduced from 0.86 ± 0.04 in M1 to 0.51 ± 0.12 in M1+SOCS (Figure 1a). The M0 versus M0+SOCS groups had comparable results to the 24 h stimulation time point, with M0 being at 0.08 ± 0.07 iNOS⁺/DAPI⁺ cells and SOCS1-KIR treatment marginally increasing that count to 0.13 ± 0.03 (Figure 1a). SOCS1-KIR peptide treatment at the 72 h stimulation time point increased iNOS⁺/DAPI⁺ cell count in the M0 macrophages from 0.12 ± 0.06 to 0.31 ± 0.06 (Figure 1a). The normalized iNOS⁺ cells reduced from 0.51 ± 0.12 in M1 macrophages to 0.26 ± 0.12 in SOCS1-KIR treated M1 macrophages (Figure 1a). Statistical significance was measured by performing a one-way ANOVA with Tukey's comparison tests ($p < 0.05$). At both 48 and 72 h, iNOS expression was significantly reduced in SOCS1-KIR treated M1 stimulated macrophages.

Across each time point represented in Figure 1a, inhibition of M1 activation, assumed as a consequence of iNOS reduction, was significantly pronounced at 24 and 48 h. At 24 h the difference in M0 groups with and without SOCS1-KIR treatment was 0.02 ± 0.004 iNOS⁺/DAPI⁺ cell count (Figure 1a). The same difference at 48 h was 0.05 ± 0.03 and 0.19 ± 0.04 at 72 h (Figure 1a), with 72 h being significant. Although the differences are minimal, we can speculate increase in iNOS expression in unstimulated M0 macrophages at 72 h to be due to the links between focal adhesion kinases (FAK) and iNOS. FAK acts a bridge between iNOS and filamentous actin (F-actin). Under hypoxia, iNOS and F-actin do not remain linked, therefore increase in FAK does not affect iNOS expression.^[39] FAK upregulation may have caused an increase in iNOS expression. The KIR region of SOCS proteins have also been shown to interact with FAK.^[40] Figure S1 (Supporting Information) displays changes in vinculin and FAK expression following SOCS1-KIR peptide treatment in M0, M1, and M2 macrophages. Although a discernable difference can be observed with SOCS treatment, the exact mechanism behind these alterations is yet to be evaluated. Investigating the exact mechanism of interactions between FAK and SOCS1-KIR as it pertains to macrophage function may be conducive to exploring the peptide's effects further.

To understand the effects of SOCS1-KIR in M1 macrophages across the time points investigated, we analyzed Cohen's d -value across each time point (Figure 1b). Cohen's d -value measures population shifts between groups, independent of the number of data points.^[41,42] In this work, we have used effect size calculations to assess the response of iNOS⁺ macrophages in the presence of SOCS1-KIR. The larger the Cohen's d value, the larger the effect size.^[42] Figure 1b shows that at 24 h SOCS1-KIR peptide was most effective in reducing iNOS⁺ cells. The effect size was 2.57 at 24 h. The effect of SOCS1-KIR on inhibition of M1 macrophages by reducing iNOS⁺ cells decreased over time. At

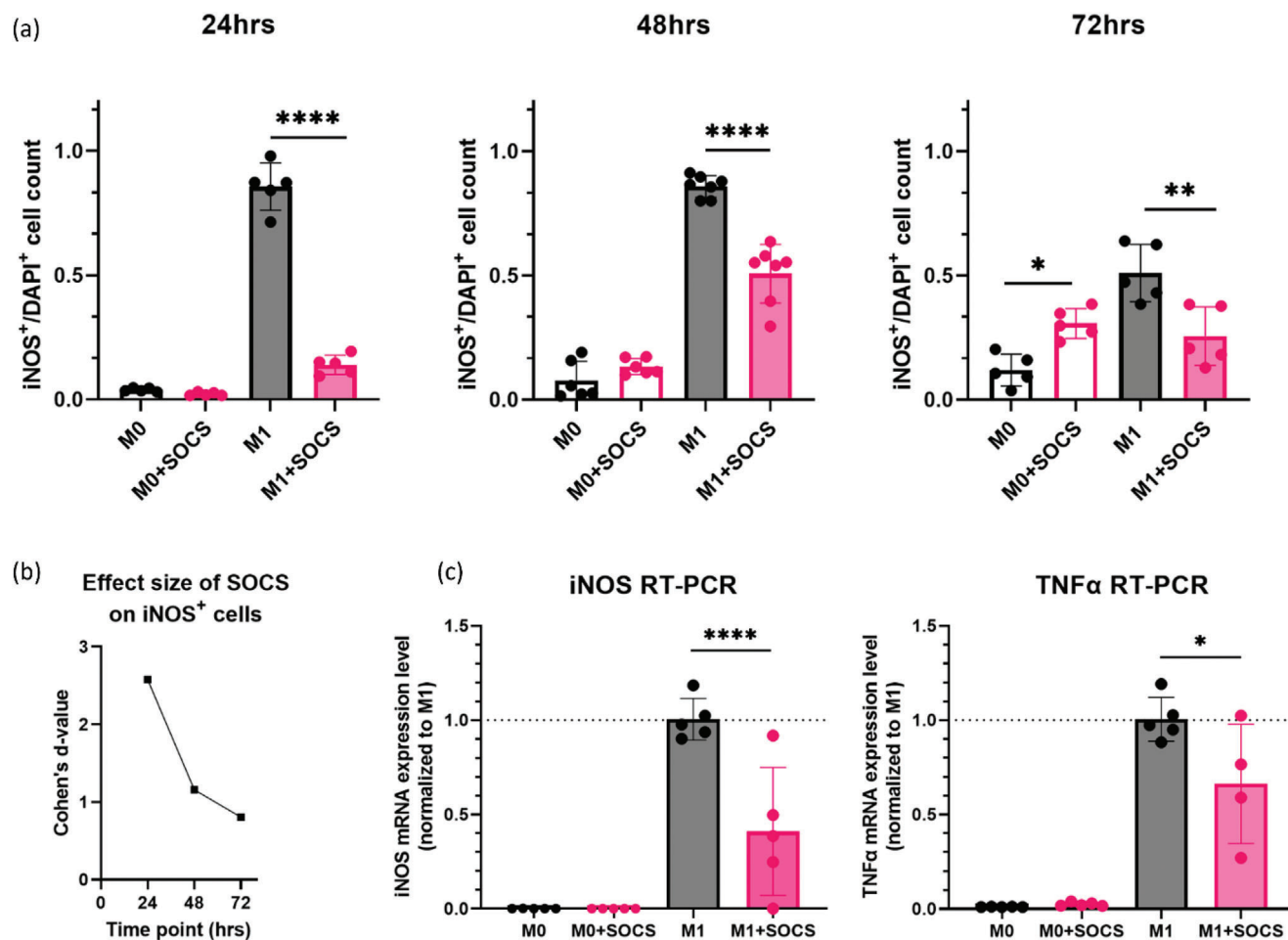


Figure 1. SOCS1-KIR peptide 2D treatment significantly reduces pro-inflammatory markers in murine macrophages. a) Image quantification of iNOS (M1 marker) expression per total DAPI (nuclei marker) positive cells immunofluorescent stained macrophages with and without SOCS1-KIR treatment at 24, 48, and 72 h. One-way ANOVA with Tukey's post hoc tests revealed that SOCS1-KIR treatment significantly reduced iNOS expression ($n = 5$; $**p < 0.01$; $****p < 0.0001$). b) Effectivity of SOCS1-KIR in reducing iNOS expression at different time points assessed by Cohen's d -value. Effect size of SOCS reduces with time. c) SOCS1-KIR peptide treatment reduces iNOS and TNF α pro-inflammatory gene expression in M1 macrophages 48 h post-stimulation. Expression values were calculated using the $2^{-\Delta\Delta C_t}$ method in which groups with SOCS1-KIR treatment are compared to Ct values obtained in M1 macrophages and normalized to the Ct values of Rplp0 housekeeping gene. One-way ANOVA with Tukey's post hoc was performed for statistical analysis. ($n = 5$; $*p < 0.05$; $****p < 0.0001$).

48 h, the d -value was 1.16, followed by the d -value being 0.81 at 72 h. Although SOCS1-KIR reduces iNOS expression at each time point, Figure 1b suggests that at 72 h in 2D, the differences in its effectivity become smaller. It is important to note that total cell count denoted by DAPI count per view field was not significantly different for any time point (Figure S2, Supporting Information). Additionally, an experiment was performed to interrogate whether treating macrophages with SOCS1-KIR after M1 stimulation would bring any changes to the trends observed (Figure S3, Supporting Information). Data indicate that the same trends follow and that although pre-peptide treatment is preferred, it may not always be necessary.

To corroborate the evidence of iNOS reduction by SOCS1-KIR, we performed RT-PCR for iNOS and TNF α on murine M1 stimulated and unstimulated M0 macrophages. TNF α is one of

the most prominent pro-inflammatory markers.^[17,19,43–44] Additionally, TNF α is robustly expressed by M1 macrophages.^[44,45] Both iNOS and TNF α (Figure 1c) were significantly reduced with SOCS1-KIR treatment in M1 macrophages. Normalized to M1, iNOS fold change was 1.01 ± 0.11 in M1 macrophages compared to 0.49 ± 0.34 in SOCS1-KIR treated M1 macrophages. TNF α fold change expression was reduced to 0.66 ± 0.32 in SOCS1-KIR treated M1 macrophages from 1.01 ± 0.12 in untreated M1 macrophages. Because all Ct values were obtained by comparing to the M1 untreated group, fold change expressions for iNOS and TNF α were negligible for M0 macrophages with and without SOCS1-KIR. Overall, expression of both pro-inflammatory markers in the M1 groups were significantly reduced with addition of 33 μM SOCS1-KIR peptide dimer in 2D cultures of murine macrophages.

3.2. SOCS1-KIR Reduces Pro-Inflammatory Factors in 2D Cultures of Human Monocyte-Derived Macrophages

To confirm translatability of our results to human, we conducted experiments in human PBMC derived macrophages. Differentiated macrophages were treated with SOCS1-KIR for 2 h after which they were stimulated to the M1 phenotype with LPS and IFN γ . As with murine macrophages, similar analyses were performed with the 2D human macrophage cultures. Since the statistical relevance of 24 and 48 h were comparable in 2D murine cultures (Figure 1), 48 h was deemed an ideal time point for SOCS1-KIR treatment in 2D human cultures.^[24,46,47] The cell supernatant or conditioned media was collected to perform a cytokine array ELISA to assess cytokine secretions (Figure S4, Supporting Information). A Nanostring gene expression assay was performed to quantify mRNA expression of myeloid genes. The Nanostring nCounter panel Myeloid Innate Immunity V2 was utilized to measure differentially expressed genes from isolated RNA of human macrophages with and without SOCS1-KIR treatment. This study is the first to profile genetic responses to SOCS1-KIR peptide treatment on human macrophages. We compared M0 and M1 macrophages with and without SOCS treatment at 48 h post-stimulation. **Figure 2a** represents the differentially expressed genes in groups with no SOCS1-KIR treatment compared to SOCS1-KIR treatment (SOCS groups are the baseline). M0 and M1 macrophages were coupled against SOCS1-KIR treated M0 and M1 macrophages. Endogenous SOCS1 proteins have been shown to upregulate M2 markers.^[17,48] This is reflected in the volcano plot (Figure 2a) as most genes upregulated with SOCS1-KIR peptide treatment were M2 related genes. The gray line is the adjusted *p*-value of 0.50. The data demonstrate trends in downregulation of M1 genes and upregulation of M2 genes with SOCS1-KIR treatment.

Among the differentially expressed or upregulated genes (represented in red dots) the mitogen-activated protein kinase 1 (MAP2K1) gene or the MEK1/2 pathway has been identified as a key regulator in pro-inflammatory M1 macrophage inhibition.^[49] Alternatively, MAP2K1 inhibition increases expression of M2 macrophage markers. The Nanostring data showed that MAP2K1 was differentially expressed in groups containing SOCS, suggesting that SOCS was reducing M1 activation. Further, a pronounced higher expression of CD163 and Fc γ RIIIA encoded gene FCGR3A (CD16a) signified an increase in M2 macrophage markers.^[50,51] V-Set Immunoregulatory Receptor (VSIR) is involved in the negative regulation of cytokine production. The upregulation of VSIR indicates that SOCS1-KIR is enabling its function in inhibiting the production of inflammatory cytokines. Similarly, all other genes listed in the volcano plot such as Mer receptor tyrosine kinase (MerTK),^[41] gluconeogenic enzyme fructose 1,6-bisphosphatase 1 (FBP1),^[52] etc. are indicators that SOCS1-KIR treatment inhibits M1 activation. These data suggest that not only does SOCS1-KIR peptide reduce pro-inflammatory M1 activation, but it may also shift the macrophage population to the anti-inflammatory M2 phenotype.

Prominent pro-inflammatory markers such as certain clusters of differentiation and tumor necrosis factor related genes are plotted in bar charts (Figure 2b). CD86 is involved in the pathogenesis of inflammation,^[43] and CD38 has been found to be upregulated in M1 macrophages.^[54] In that regard, both

CD86 and CD38 gene expression were reduced with SOCS1-KIR treatment (Figure 2b) as represented by the normalized log₂ fold change values. Genes encoding the TNF gene family such as TNF α -induced protein (AIP)-3,6, TNFS4, and TNF receptor superfamily (RSF)-8,1B,14 are also plotted in bars as log₂ fold change values. SOCS1-KIR treatment reduced previously listed TNF family genes. Heatmaps were created from pathways such as IFN signaling, cytokine signaling, JAK/STAT signaling, and chemokine signaling. The normalized log₂ gene expression values of M0 and M1 with and without SOCS1-KIR treatment were mapped for genes of interest (Figure 2c). SOCS1-KIR peptide treatment reduced expression of pro-inflammatory genes in M1 stimulated macrophages while the M0 macrophages acted as controls (Figure 2c). Figure 2c represents genes upregulated by LPS and IFN γ stimulations for activating the M1 phenotype. Some examples of those genes are interleukin (IL)-1B, IL-6, hypoxia inducible factor 1 alpha (HIF1A), toll-like receptor 4 (TLR4), IL-12A, nuclear factor kappa B (NF κ B), etc. The normalized log₂ values displayed a downregulation in M1 related genes with SOCS1-KIR treatment as indicated by dark purple for high expression and light yellow for low expression. Arachidonate 5-lipoxygenase activating protein (ALOX5AP) is expressed by M1 macrophages upon activation.^[55] There was a clear reduction in the expression of ALOX5AP signifying a reduced state of M1 activation. Chemokine ligand 1 (CXCL1) and CXCL9 have been shown to be downregulated with treatment of steroids in chronic inflammatory disorders such as ulcerative colitis.^[56] A reduction in the mRNA expression of CXCL1 and CXCL9 suggests that SOCS1-KIR peptide has inhibitory effects in M1 macrophage activation. Figure 2c also represents a heatmap of the normalized log₂ counts for genes encoding the JAK/STAT pathway such as SOCS1 and SOCS3. Interferon regulatory factors manage macrophage polarization by activation of the JAK/STAT pathway.^[57–59] Particularly, interferon regulatory factor (IRF) 4 and IRF 7 regulate IFN production.^[60]

The mRNA expressions of genes encoding cytokines assessed via ELISA (Figure S4, Supporting Information) are demonstrated in the heatmap (Figure 2c). IFNGR1 is a receptor for IFN γ , TNFRSF1B and TNF encode TNF α , chemokine ligand 2 (CCL2), a primary ligand for CCR2 is the gene for MCAF, and colony stimulating factor 2 (CSF2) encodes GM-CSF. All gene expression values were downregulated with SOCS1-KIR peptide treatment in M1 macrophages. This data corroborated with the ELISA study (Figure S4, Supporting Information) indicating that SOCS1-KIR reduced expression of both secreted proteins and downstream mRNA expressions in M1 macrophages. A reduction in the expression of these genes indicated that pro-inflammatory markers were being reduced with SOCS1-KIR treatment. The regulation of genes is well known in the fate of T helper cells,^[50] but not much is known about the affected pathways involving macrophages. The Nanostring data provide insight into which genes, chemokine and cytokine receptors are up or downregulated with SOCS1-KIR peptide treatment in human macrophages. Overall, the heatmaps demonstrate that SOCS1-KIR peptide dimer can function effectively in reducing M1 macrophage activation with human monocyte derived macrophages and may even potentially increase M2 activation. Further, representations of the cellular signaling pathways with SOCS1-KIR treatment have also been demonstrated

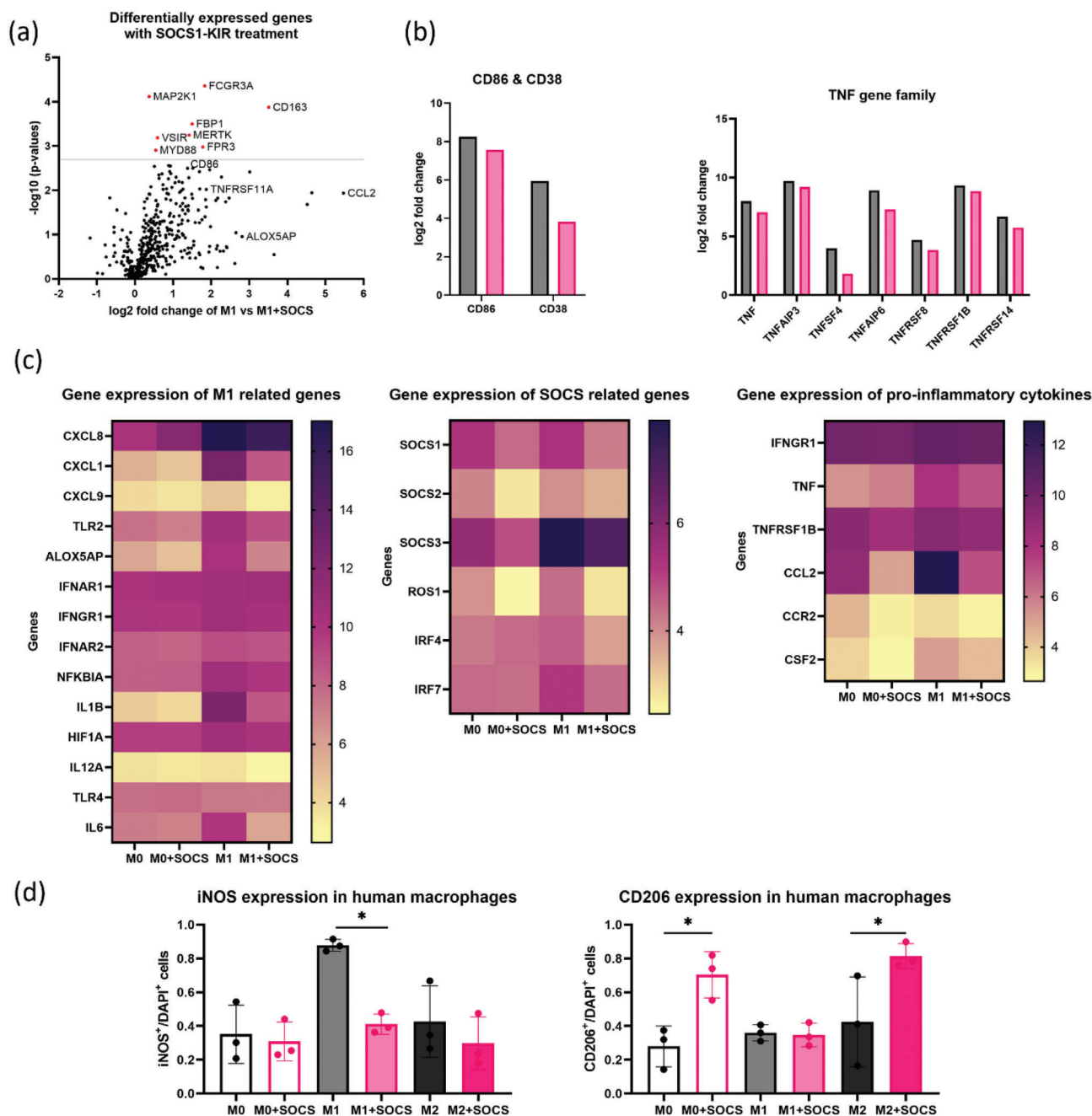


Figure 2. SOCS1-KIR peptide treatment reduces pro-inflammatory profile of human macrophages 48 h post-stimulation in 2D. a) Volcano plot of differentially expressed or upregulated genes (red dots) via Nanostring. Only differentially expressed genes ($p < 0.50$) were represented in the volcano plot. The gray line represented a p -value of $p < 0.50$. b) Prominent pro-inflammatory genes such as CD86, CD38, and the TNF gene family (represented in bar plots) are downregulated following SOCS1-KIR treatment. c) SOCS1-KIR treatment downregulated expression of pro-inflammatory genes in additional M1 macrophage related genes, SOCS related genes, and genes encoding pro-inflammatory cytokines. The normalized log₂ gene expression values were plotted for M0 and M1 macrophages with and without SOCS1-KIR treatment. d) Quantifying iNOS (M1 associated) expression per total DAPI (nuclei marker) positive cells, and CD206 (M2 associated) expression per total DAPI positive cells via immunostaining in human macrophages following SOCS1-KIR treatment for 48 h. SOCS treatment reduced iNOS⁺ M1 macrophages and increased CD206⁺ M0 and M2 treated SOCS groups. Statistical significance was measured by one-way ANOVA with Tukey's post hoc tests ($n = 3$; $*p < 0.05$).

in Figures S5–S7 (Supporting Information). In the pathway analysis charts, SOCS1-KIR peptide clearly displays a downregulation of inflammatory signaling via inhibition of STAT recruitment in the JAK-STAT signaling pathway (Figure S5, Supporting Information), downregulation of STAT signaling, NF κ B expres-

sion and TNF related markers in the chemokine signaling pathway (Figure S6, Supporting Information), and the TNF signaling pathway (Figure S7, Supporting Information) respectively.

In addition to gene expression studies and assessing secreted cytokines with SOCS1-KIR treatment in human macrophages,

immunostaining was also performed. Macrophages were fixed and stained for iNOS, CD206, and DAPI after 48 h. CD206, a mannose receptor is a prominent marker for M2 macrophages. Since the upregulated genes in the volcano plot could be associated to M2-like macrophages, we investigated the effects of SOCS1-KIR peptide on M2 activation via immunostaining. CD206 expression per total DAPI positive cells was assessed alongside iNOS expression. Immunofluorescent images of macrophages treated with and without SOCS1-KIR were captured and quantified. A one-way ANOVA revealed that following SOCS1-KIR treatment, iNOS expression was significantly reduced in M1 stimulated macrophages (Figure 2d), and that CD206 expression was increased in M0 and M2 macrophages. M1 macrophage count for iNOS⁺ cells per total DAPI⁺ cells, was 0.87 ± 0.03 without SOCS1-KIR. While SOCS1-KIR treated M1 macrophages had a reduction to 0.41 ± 0.06 iNOS⁺ cells per total DAPI⁺ cells. The reduction in iNOS expression of M0 macrophages was not significantly different as it reduced from 0.35 ± 0.17 to 0.31 ± 0.12 iNOS⁺/DAPI⁺ cells. Similarly, the differences in iNOS expression of M2 macrophages had a minimal difference from 0.43 ± 0.21 without SOCS to 0.29 ± 0.15 with SOCS treatment. On the other hand, SOCS1-KIR treatment had no significant effects on CD206 expression for M1 macrophages. The CD206 per total DAPI positive cells quantification was 0.36 ± 0.05 for untreated M1 macrophages and 0.35 ± 0.07 for SOCS treated M1 macrophages. This was expected as M1 macrophages do not express the CD206 mannose receptor.

M0 and M2 macrophages were significantly upregulated for CD206 expression with SOCS1-KIR treatment. The expression for CD206 increased from 0.28 ± 0.12 to 0.70 ± 0.14 for SOCS treated M0 macrophages. M2 macrophages with SOCS1-KIR treatment demonstrated almost a twofold increase of CD206⁺ cells with CD206 per total DAPI positive values being 0.42 ± 0.26 with no SOCS1-KIR and 0.81 ± 0.07 in the presence of SOCS1-KIR. These results corroborate with the results obtained from the gene expression analysis of a human macrophage panel. This study is the first to enlist Nanostring gene expression to investigate the alterations occurred by SOCS1-KIR peptide treatment on human macrophages. It can be inferred that while SOCS1-KIR reduces iNOS expression, it may also be shifting the macrophage phenotype from pro-inflammatory M1 to an anti-inflammatory M2-like macrophages.

Further, release of pro-inflammatory cytokines such as IFN γ , TNF α , monocyte chemotactic protein-1 (MCP-1 or MCAF) and GM-CSF were analyzed through collection of cell supernatant and quantification of soluble proteins (Figure S4, Supporting Information). IFN γ is a cytokine well known for skewing macrophages to the pro-inflammatory phenotype.^[61] We found SOCS1-KIR treatment displayed a trend in reduction of IFN γ secretion from 27.54 to 11.63 pg mL⁻¹ in M1 macrophages (Figure S4, Supporting Information). TNF α is another prominent inflammatory cytokine that plays a major role in initiating the immune response by releasing a cytokine cascade thereby recruiting macrophages to the site of infection.^[62] SOCS1-KIR treatment in M1 macrophages reduced TNF α secretion from 456.8 to 358.8 pg mL⁻¹. A reduction in TNF α expression via RT-PCR of murine macrophages (Figure 1c) and ELISA of human macrophage supernatant (Figure S4, Supporting Information) signifies that SOCS1-KIR reduced TNF α in both groups.

Similarly, MCAF enhances phagocytosis and accelerates recruitment of macrophages.^[63] MCAF secretion reduced from 1080.58 pg mL⁻¹ in M1 macrophages to 181.41 pg mL⁻¹ in SOCS1-KIR treated M1 macrophages (Figure S4, Supporting Information). A reduction in MCAF suggests that M1 macrophages were not being activated in the presence of SOCS1-KIR. GM-CSF plays a critical role in differentiation and proliferation of myeloid cells such as neutrophils and macrophages.^[64] Along with recruiting and activating macrophages, the production of GM-CSF is critical to maintaining a balanced healing cascade. Inversely, an imbalance in GM-CSF production can lead to chronic inflammatory conditions.^[65] The trends in Figure S4 (Supporting Information) demonstrated a reduction in the secretion of GM-CSF in M1 macrophages treated with SOCS1-KIR from 1762.41 to 1496.58 pg mL⁻¹. A reduced GM-CSF concentration signifies that SOCS1-KIR caused a hindrance to M1 macrophage activation. The ELISA study demonstrated trends that all pro-inflammatory cytokines were reduced in M1 macrophages with SOCS1-KIR treatment.

3.3. Determination of SOCS1-KIR Peptide's Retention in PEGDA-SOCS Hydrogel

PEG, a polyether with hydrophilic, bioinert, minimally immunogenic properties, has resulted in numerous applications for pharmaceutical formulations.^[66,67] Due to their high water content, excellent solubility, and hydrophilicity, PEGDA hydrogels offer note-worthy resemblance to natural living tissue, which is highly beneficial for in vitro analyses and applications.^[68] With relatively simple chemistry, PEGDA hydrogels can incorporate bioactive components to create a biomimetic environment for cells.^[69] PEG hydrogels or scaffolds for clinical applications can be modified by altering the weight percentage of PEG to allow some degree of protein adsorption and/or adding bioactive peptides. Herein this work, we use PEGDA hydrogels to encapsulate SOCS1-KIR for macrophage manipulation.

Figure 3a represents a schematic of the control or PEG-RGDS, and the PEGDA-SOCS hydrogels wherein each componential design is enlisted to demonstrate how the hydrogels were formed. Concentration of peptides, PEG molecular weight, and polymer density can be altered to modulate mesh size and the rate of protein release. Depending on the mesh size of a hydrogel network, the protein may or may not be released in the exterior environment.^[70] We analyzed the hydrogel characteristics to determine SOCS retention in the hydrogel formulation.

A BCA assay was conducted to assess retention or release of SOCS1-KIR in the environment (Figure S8a, Supporting Information). The three hydrogel groups compared were PEGDA only, PEG-RGDS, and PEG-SOCS or SOCS hydrogel. The PEGDA used in our hydrogel system was 10 kDa in size, PEG-RGDS was nearly 3833 Da and the SOCS1-KIR peptide dimer was 4752 Da. The concentrations of released proteins were quantified over an iterative sample collection for 7 days (Figure S8b, Supporting Information) and absorbance was measured at 562 nm. To negate any perceived signal from residual eosin Y/NVP, its concentrations were also measured separately. Over 7 days, concentration of PEGDA was 121.6 ± 17.42 μ g mL⁻¹, PEG-RGDS was 134.6 ± 18.87 μ g mL⁻¹, and PEG-SOCS was 143.2 ± 28.61 μ g mL⁻¹.

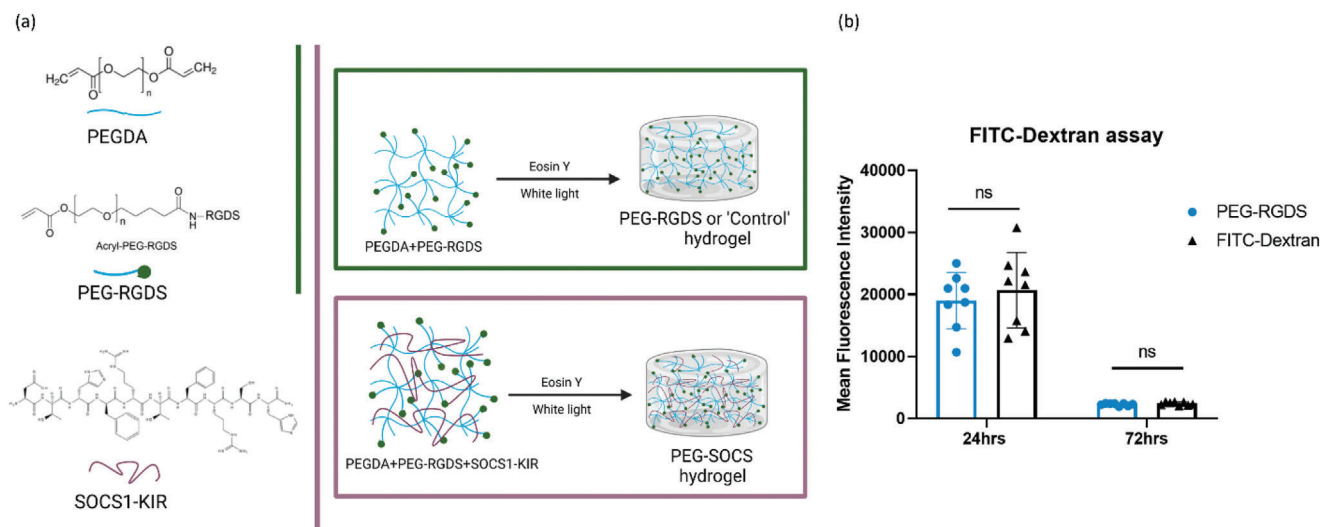


Figure 3. SOCS1-KIR is retained in the hydrogel. a) Schematic of the control or “PEG-RGDS” hydrogel and the experimental or “PEG-SOCS” hydrogel. b) To investigate SOCS1-KIR release or retention following encapsulation in the hydrogel, FITC-Dextran was used as a surrogate protein. Mean fluorescence intensity was assessed via a FITC-Dextran diffusion test to measure release or retention of FITC-Dextran from the hydrogel ($n = 8$ hydrogels). Student's t -test indicated non-significant difference at 24 or 72 h following encapsulation ($p < 0.05$).

(Figure S8b, Supporting Information). Overall concentration of eosin Y was $137 \pm 14.81 \mu\text{g mL}^{-1}$. On comparing differences of concentrations of the hydrogel groups to eosin Y, only a nominal amount of protein was being released from the SOCS gels through 7 days ($\approx 6.2 \mu\text{g mL}^{-1}$). From days 1–4, the PEG-SOCS hydrogel trended slightly higher in protein content, i.e., $20.6 \mu\text{g mL}^{-1}$, when normalized to eosin Y, albeit not significantly higher than other groups. PEG-RGDS concentration after eosin Y normalization was $10.3 \mu\text{g mL}^{-1}$ and PEGDA values were negative. After day 4, all trends seem to be similar. Due to extremely low protein concentrations at the start of forming hydrogels, the data present some variability. Since day 2 (24 h) and day 4 (72 h) showed more variability amongst all groups (from Figure S8b, Supporting Information) concentrations at 24 and 72 h were reported in Figure S8a (Supporting Information). At 24 h, eosin Y was $147.4 \mu\text{g mL}^{-1}$, PEGDA was $145.7 \mu\text{g mL}^{-1}$, PEG-RGDS was $151.2 \mu\text{g mL}^{-1}$, and PEG-SOCS was $183.2 \mu\text{g mL}^{-1}$. At 72 h, eosin Y was $126.5 \mu\text{g mL}^{-1}$, PEGDA was $115.7 \mu\text{g mL}^{-1}$, PEG-RGDS or “control” was $111.3 \mu\text{g mL}^{-1}$, and PEG-SOCS was $112.6 \mu\text{g mL}^{-1}$. A one-way ANOVA with Tukey's post-hoc test was performed to assess statistical significance ($p < 0.05$). No statistical significance was found between the groups. Considering the variability in profiles, and no statistical difference between each group, it can be inferred that majority of the SOCS1-KIR peptide is being retained in the hydrogel over 7 days. Any protein release from PEGDA and PEG-RGDS hydrogels was also negligible when compared to eosin Y/NVP. The retention of SOCS1-KIR in the hydrogel environment is beneficial to avail its macrophage inhibiting properties for macrophages encapsulated within the PEGDA hydrogel.

To ensure no changes to bulk properties of the hydrogel occurred after incorporation of SOCS1-KIR in the hydrogel network, a swelling test was performed. Swelling was determined by calculating swelling ratio of the two groups. PEG-SOCS hydrogels demonstrated a higher swelling ratio of 1.13 ± 0.39 com-

pared to 0.92 ± 0.34 for control hydrogels, although they were not significantly different to each other (Figure S9a, Supporting Information). The swelling test confirmed that SOCS1-KIR being entrapped in the hydrogel network does not significantly influence the swelling ratio of the hydrogel. It can be inferred that SOCS1-KIR peptide was not a hindrance to diffusion of proteins through the hydrogel while macrophages were in culture. If needed, ratios of PEGDA to SOCS1-KIR can be varied to manipulate porosity or permeability of the hydrogels.^[71,72] The gelation chemistry and the composition of our hydrogels can also be modified to allow for rapid release of the peptide in the external environment, if release is desired. However, since macrophages are encapsulated in the hydrogel along with SOCS1-KIR, the expectancy of SOCS1-KIR release is nominal.

To further probe if the PEG-SOCS hydrogel design can model as a therapeutic allowing retention of other moieties in the gel, a FITC-Dextran experiment was performed. Comparable molecular weight of FITC conjugated Dextran (≈ 4 kDa) was used as a surrogate for the SOCS1-KIR peptide. Figure 3b demonstrates that there was negligible release of FITC-Dextran out of the hydrogel. Mean fluorescence intensity (MFI) for an additional control, i.e., eosin Y in solution, and FITC-Dextran in solution was also measured (Figure S9b, Supporting Information). MFI of FITC-Dextran at 24 h was 20703 ± 733.5 compared to 19011 ± 683.12 for control hydrogel. At 72 h, the MFI reduced to 2412 ± 75.75 for FITC loaded hydrogels versus 2264 ± 116.5 for control hydrogels. Figure 3b demonstrates that the current hydrogel design can retain FITC-Dextran at the same concentration that SOCS1-KIR was retained.

SOCS1-KIR peptide houses an N-terminal palmitoyl group that allows passive diffusion through the cell membrane. SOCS1-KIR retention in the hydrogel benefits our system as macrophages that are encapsulated within the hydrogel environment and can be directly exposed to the peptide. A non-significant release may be observed due to a small mesh size

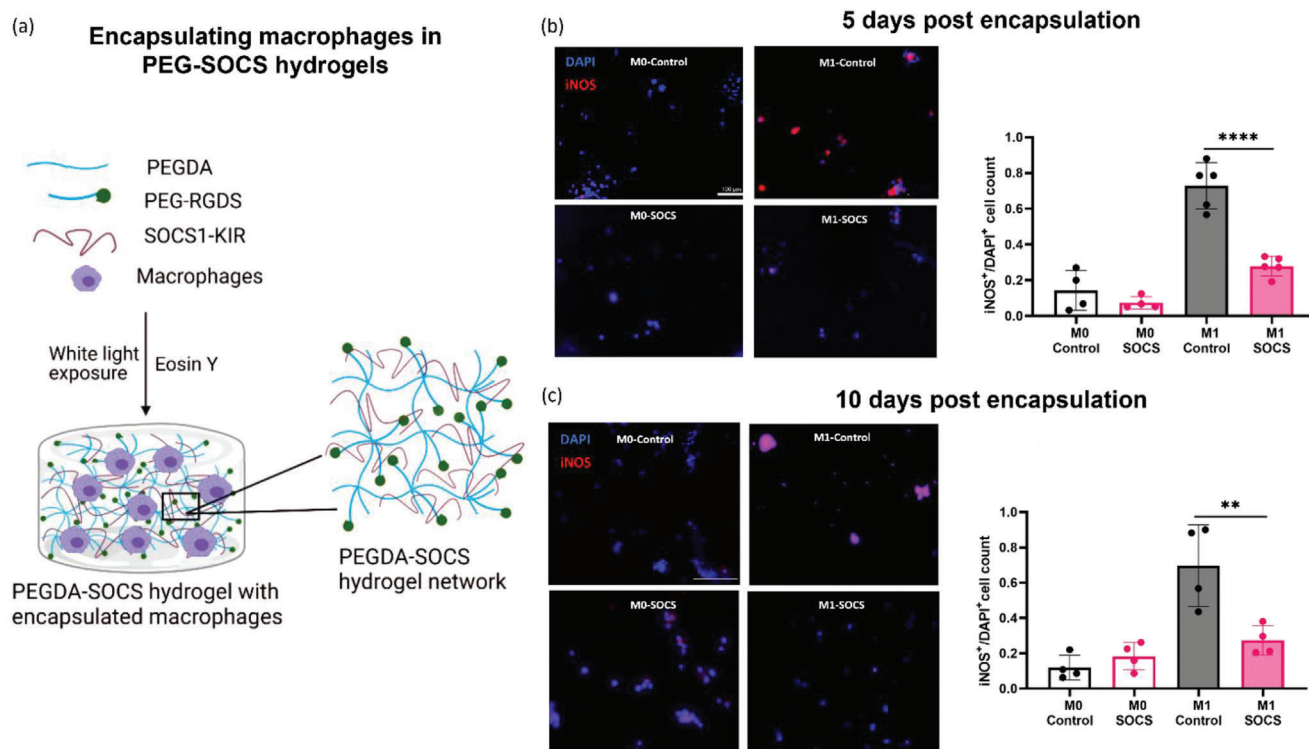


Figure 4. SOCS1-KIR peptide in a PEG hydrogel reduces iNOS expression in murine macrophages. a) Schematic for the encapsulation of macrophages in the PEGDA-SOCS (or PEG-SOCS) hydrogel. Immunofluorescent images of DAPI (blue, nuclei marker) and iNOS (red, M1 macrophage marker) stained macrophages in control and SOCS hydrogels. Quantification of iNOS expression per total DAPI positive cells in macrophages encapsulated in control and SOCS hydrogels. b) $n = 5$ gels for 5 days post encapsulation. c) $n = 4$ gels for 10 days post encapsulation. One-way ANOVA demonstrated a reduction in iNOS expression of murine macrophages encapsulated in SOCS hydrogels (Scale = 100 μ m; ** $p < 0.01$; **** $p < 0.0001$).

of the crosslinked network of the PEG-RGDS control hydrogel. Utilizing the Flory Rehner equation, an estimate mesh size of the PEGDA hydrogel was calculated to be 3.17 nm (refer to Equations (S2) and (S3), Supporting Information for calculations). This mesh size was in accordance with values found from literature.^[73–75,79] The SOCS1-KIR peptide interspersed within the hydrogel blocks JAK kinase activity via its KIR region. At the same time, the cell membrane-penetrating palmitated group in SOCS1-KIR is unobstructed as this region is not covalently conjugated to PEGDA.^[76,77] The N terminal palmitoyl-lysine group is advantageous to our system as we hypothesize that encapsulated macrophages can interact with the entrapped SOCS1-KIR peptide in the hydrogel environment.

3.4. SOCS1-KIR in a PEG Hydrogel Reduces Pro-Inflammatory Murine Macrophage Markers

To prevent pro-inflammatory macrophage activation, we encapsulated SOCS1-KIR peptide mimetic in a PEGDA hydrogel platform. Our work focused on utilizing the SOCS1-KIR peptide to create a biofunctional PEG-based hydrogel platform that can be leveraged to reduce macrophage inflammation.

To create a hydrogel system for presenting SOCS1-KIR peptide as an M1 inhibitor, PEGDA was crosslinked with conju-

gated PEG-RGDS, and SOCS1-KIR peptide. Encapsulation of macrophages occurred by mixing the cells with the macromers and together, the cell-polymer solution was exposed to eosin Y and white light (Figure 4a). Designing such hydrogels with biologically derived peptides either covalently bound or entrapped in synthetic polymer networks facilitates improvement in cell compatibility, protein release by tuning of network properties, and exploiting the properties of one or more of the polymers in the system.^[78]

For the 3D encapsulation studies, there were two main groups of hydrogels—“control” (PEGDA+PEG-RGDS) hydrogels and experimental (PEGDA+PEG-RGDS+SOCS1-KIR) or “PEGDA-SOCS/PEG-SOCS” or SOCS hydrogels. Murine macrophages were encapsulated in control and SOCS hydrogels ($n = 4$ or 5) for 5 days (Figure 4b) and 10 days (Figure 4c). All samples were fixed for staining and quantification of iNOS expression. Figure 4b,c demonstrate iNOS⁺/DAPI⁺ images of M0 and M1 macrophages encapsulated in control and PEG-SOCS gels at both the 5-day and 10-day time point, respectively. A one-way ANOVA reveals a significant reduction of iNOS expression per total DAPI cell count for M1 macrophages encapsulated in the PEG-SOCS hydrogels. At 5 days (Figure 4b), iNOS⁺/DAPI⁺ values decreased from 0.73 ± 0.13 for M1 macrophages in control hydrogels to 0.28 ± 0.05 in SOCS hydrogels. iNOS expression was not significantly different for M0 macrophages, as the values reduced

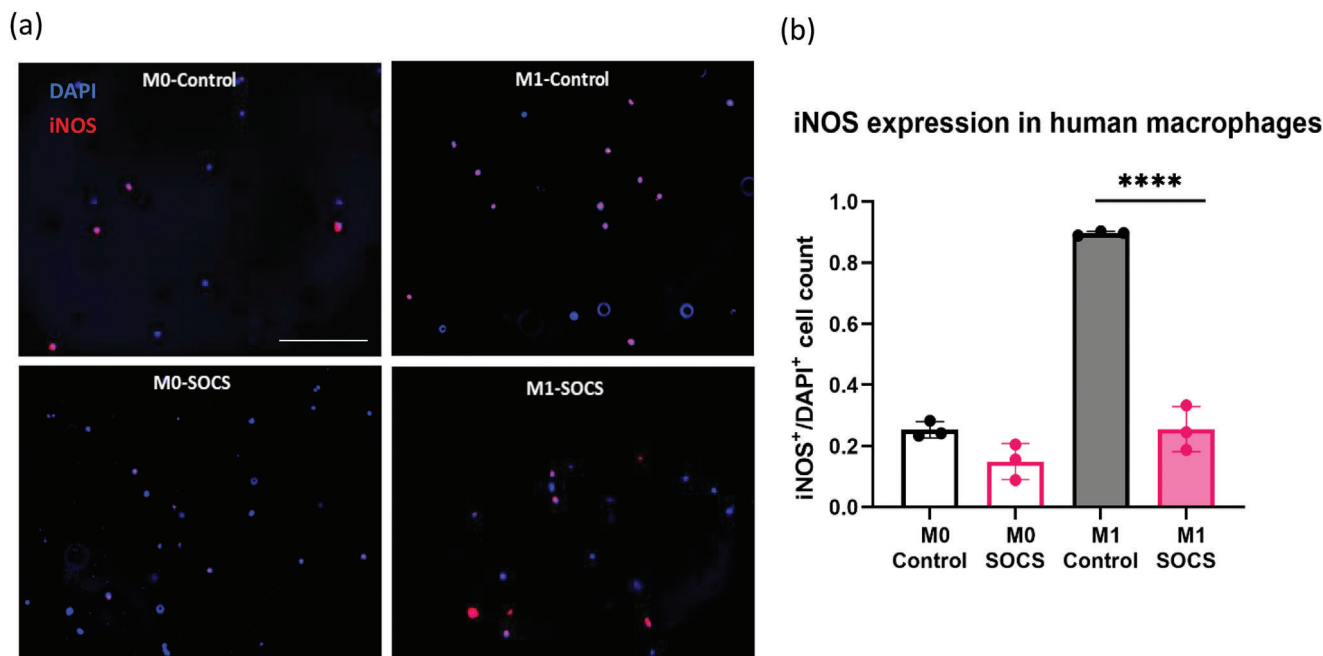


Figure 5. SOCS hydrogels reduce iNOS expression in human macrophages. a) Immunofluorescent images of iNOS expression per total DAPI positive cells of human macrophages encapsulated in SOCS hydrogels ($n = 3$; Scale = 100 μm). b) A one-way ANOVA confirmed significant reduction in iNOS expression per total DAPI positive cells of human macrophages encapsulated in SOCS hydrogels ($n = 3$, **** $p < 0.0001$).

from 0.14 ± 0.11 in control hydrogels to 0.07 ± 0.03 following encapsulation in SOCS hydrogels. At 10 days (Figure 4c), the differences in iNOS⁺/DAPI⁺ encapsulated M0 macrophages was minimal. M0 macrophages encapsulated in control hydrogels had a value of 0.12 ± 0.7 whereas values for SOCS hydrogel encapsulated M0 macrophages were 0.18 ± 0.07 . There is a significant reduction of iNOS expression from 0.69 ± 0.23 for M1 macrophages encapsulated in control hydrogels to 0.27 ± 0.08 for M1 macrophages encapsulated in PEG-SOCS hydrogels. Replacing all M1 media with M0 media on day 5 caused a change in the environment of encapsulated macrophages. Hence, the 10-day time point aided in observing the long-term inhibitory effects of SOCS1-KIR in the 3D hydrogel system. Encapsulation in PEG-SOCS hydrogels did not affect total cell count (Figure S10, Supporting Information). The reduction in iNOS expression of macrophages encapsulated in SOCS hydrogels was comparable to the change observed in 2D cultures of SOCS1-KIR treated macrophages. At 5 days, the difference between the averages of iNOS expression of M1 macrophages in PEG-SOCS versus control hydrogel was 0.45, and at 10 days that difference of averages was 0.42. The difference of averages in iNOS expression of SOCS1-KIR treated 2D cultured murine macrophages was 0.71 at 24 h, 0.35 at 48 h, and 0.25 at 72 h. The experimental timeline of the 5-day experiment in 3D is similar to 72 h in 2D, as exposure to SOCS1-KIR is for 72 h for both experiments. Due to similar timelines, it can be concluded that the overall efficacy of SOCS1-KIR was doubled when presented in a hydrogel formulation compared to 2D. Figure 4 exhibits the ability of SOCS1-KIR to be used in a PEGDA hydrogel for reducing M1 macrophage activation.

3.5. PEG-SOCS Hydrogel Reduces iNOS Expression in Human Monocyte Derived Macrophages

Validation of the results from the 2D encapsulation experiments were also attempted in 3D cultures of human macrophages encapsulated in SOCS hydrogels. Monocytes were differentiated to macrophages as previously explained. Differentiated macrophages were encapsulated in control hydrogels and SOCS hydrogels. The experimental design was the same as it was for the 5-day time point of 3D experiments with murine macrophages. The human macrophages were stimulated for 72 h in the hydrogel considering day 1 as the day of encapsulation, day 2 as the M1 stimulation time point, and day 5 as the day of fixing samples. The encapsulated cells in gels were fixed for immunofluorescent staining analyses 5 days post encapsulation. Figure 5 represents M0 and M1 macrophages encapsulated in control and SOCS hydrogels ($n = 3$). The overlay of DAPI (blue) and iNOS (red) channels are demonstrated in Figure 5a. Quantification of iNOS expression denoted an insignificant change in M0 macrophages. Encapsulation of untreated M0 macrophages reduced iNOS expression from 0.25 ± 0.02 to 0.14 ± 0.05 iNOS⁺ cells per total DAPI⁺ cell count (Figure 5b). SOCS hydrogels significantly reduced iNOS expression in M1 stimulated macrophages. The entrapped SOCS1-KIR peptide decreased iNOS⁺/DAPI⁺ cells in M1 macrophages from 0.89 ± 0.01 to 0.25 ± 0.07 (Figure 5b). Additionally, cell count assessed by DAPI⁺ cells across all conditions remained unaffected (Figure S11, Supporting Information). The hydrogel platform containing SOCS1-KIR peptide in a PEGDA network promises to be an effective strategy for reducing M1 activation in human macrophages. CD206 staining (not

represented) was also performed for human macrophages encapsulated in SOCS hydrogels. CD206 staining was inconclusive and no significant differences were found between any group in response to being exposed by the entrapped SOCS1-KIR peptide.

4. Conclusion

This is the first effort to utilize a hydrogel platform incorporating the SOCS1-KIR peptide to modulate macrophage function. Through our work, we successfully demonstrated the anti-inflammatory abilities of SOCS1-KIR peptide mimic on murine and human pro-inflammatory M1 macrophages. This work was the first to introduce a functionalized PEG-based hydrogel platform that incorporated the SOCS1-KIR peptide dimer. The system can successfully retain SOCS1-KIR for exposure to encapsulated macrophages as assessed via hydrogel characterization assays. Through 2D and 3D experiments, we demonstrated that the SOCS hydrogel reduced M1 macrophage activation via immunostaining, soluble cytokine secretion assays and gene expression assays. Our system elucidates how SOCS1-KIR in PEGDA hydrogels can be utilized as an effective therapeutic for macrophage manipulation.

Supporting Information

Supporting Information is available from the Wiley Online Library or from the author.

Acknowledgements

This work was financially supported by the Rhines Rising Star Larry Hench Professorship (E.M.). Under #IRB202101975 through the University of Florida Institutional Review Board, the authors purchased human monocytes to profile the human macrophage response to SOCS1-KIR. The spelling error in the title was corrected on September 14, 2023.

Conflict of Interest

The authors declare no conflict of interest.

Author Contributions

A.J.: Conceptualization, data curation, experimental design, formal analysis, methodology, visualization, writing—original draft preparation, writing-review and editing. J.L. III: resources, writing-review and editing. E.M.: methodology, experimental design, supervision, visualization, writing—original draft supervision and modification, writing-review and editing.

Data Availability Statement

The data that support the findings of this study are available from the corresponding author upon reasonable request.

Keywords

M1 activation, macrophages, PEGDA, suppressors of cytokine signaling

Received: May 25, 2023
Published online: July 9, 2023

- [1] A. C. D. O. Gonzalez, T. F. Costa, Z. D. A. Andrade, A. R. A. P. Medrado, *An. Bras. Dermatol.* **2016**, 91, 614.
- [2] S. A. Eming, P. Martin, M. Tomic-Canic, *Sci. Transl. Med.* **2014**, 6, 265sr6.
- [3] L. Chen, H. Deng, H. Cui, J. Fang, Z. Zuo, J. Deng, Y. Li, X. Wang, L. Zhao, *Oncotarget* **2018**, 9, 7204.
- [4] P. Krzyszczyk, R. Schloss, A. Palmer, F. Berthiaume, *Front. Physiol.* **2018**, 9, 419.
- [5] C. J. Ferrante, S. J. Leibovich, *Adv. Wound Care* **2012**, 1, 10.
- [6] L. A. Dipietro, T. A. Wilgus, T. J. Koh, *Int. J. Mol. Sci.* **2021**, 22, 950.
- [7] S. Gordon, *Nat. Rev. Immunol.* **2003**, 3, 23.
- [8] J. M. Daley, S. K. Brancato, A. A. Thomay, J. S. Reichner, J. E. Albina, *J. Leukocyte Biol.* **2010**, 87, 59.
- [9] M. Hesketh, K. B. Sahin, Z. E. West, R. Z. Murray, *Int. J. Mol. Sci.* **2017**, 18, 1545.
- [10] E. A. Ross, A. Devitt, J. R. Johnson, *Front. Immunol.* **2021**, 12, 3234.
- [11] S. Banerjee, A. Biehl, M. Gadina, S. Hasni, D. M. Schwartz, *Drugs* **2017**, 77, 521.
- [12] R. Morris, N. J. Kershaw, J. J. Babon, *Protein Sci.* **2018**, 27, 1984.
- [13] F. Seif, M. Khoshmirsafa, H. Aazami, M. Mohsenzadegan, G. Sedighi, M. Bahar, *Cell Commun. Signaling* **2017**, 151, 15.
- [14] C. E. Egwuagu, I. Joseph Larkin, *JAKSTAT* **2013**, 2, e24134.
- [15] N. P. D. Liau, A. Laktyushin, I. S. Lucet, J. M. Murphy, S. Yao, E. Whitlock, K. Callaghan, N. A. Nicola, N. J. Kershaw, J. J. Babon, *Nat. Commun.* **2018**, 9, 9.
- [16] M. C. Trengove, A. C. Ward, *Am. J. Clin. Exp. Immunol.* **2013**, 2, 1.
- [17] Y.-B. Liang, H. Tang, Z.-B. Chen, L.-J. Zeng, J.-G. Wu, W. Yang, Z.-Y. Li, Z.-F. Ma, *Mol. Med. Rep.* **2017**, 16, 6405.
- [18] C. S. Whyte, E. T. Bishop, D. Rückerl, S. Gaspar-Pereira, R. N. Barker, J. E. Allen, A. J. Rees, H. M. Wilson, *J. Leukocyte Biol.* **2011**, 90, 845.
- [19] I. Kinjo, T. Hanada, K. Inagaki-Ohara, H. Mori, D. Aki, M. Ohishi, H. Yoshida, M. Kubo, A. Yoshimura, *Immunity* **2002**, 17, 583.
- [20] N. Doti, P. L. Scognamiglio, S. Madonna, C. Scarponi, M. Ruvo, G. Perretta, C. Albanesi, D. Marasco, *Biochem. J.* **2012**, 443, 231.
- [21] S. Huang, K. Liu, A. Cheng, M. Wang, M. Cui, J. Huang, D. Zhu, S. Chen, M. Liu, X. Zhao, Y. Wu, Q. Yang, S. Zhang, X. Ou, S. Mao, Q. Gao, Y. Yu, B. Tian, Y. Liu, L. Zhang, Z. Yin, B. Jing, X. Chen, R. Jia, *Front. Immunol.* **2020**, 11, 558341.
- [22] J. Sharma, T. D. Collins, T. Roach, S. Mishra, B. K. Lam, Z. S. Mohamed, A. E. Veal, T. B. Polk, A. Jones, C. Cornaby, M. I. Haider, L. Zeumer-Spataro, H. M. Johnson, L. M. Morel, J. Larkin, *Sci. Rep.* **2021**, 11, 6354.
- [23] J. Sharma, J. Larkin, *Front. Pharmacol.* **2019**, 10, 324.
- [24] L. D. Jager, R. Dabelic, L. W. Waiboci, K. Lau, M. S. Haider, C. M. I. Ahmed, J. Larkin, S. David, H. M. Johnson, *J. Neuroimmunol.* **2011**, 232, 108.
- [25] A. H. Dalpke, S. Oppen, S. Zimmermann, K. Heeg, *J. Immunol.* **2001**, 166, 7082.
- [26] International Union of Pure and Applied Chemistry Macromolecular Division Commission on Macromolecular Nomenclature * Glossary of Basic Terms in Polymer Science (IUPAC Recommendations 1996), **1996**.
- [27] Y. Wu, K. Jane Grande-Allen, J. L. West, *Cell. Mol. Bioeng.* **2016**, 9, 479.
- [28] S. L. Bellis, *Biomaterials* **2011**, 32, 4205.
- [29] X. Jin, H. S. Kruth, *J. Vis. Exp.* **2016**, 54244, 2016.
- [30] E. B. Peters, N. Christoforou, K. W. Leong, G. A. Truskey, J. L. West, *PolyCell. Mol. Bioeng.* **2015**, 9, 38.
- [31] B. K. Mann, A. S. Gobin, A. T. Tsai, R. H. Schmedlen, J. L. West, *Biomaterials* **2001**, 22, 3045.
- [32] L. Parisi, E. Gini, D. Baci, M. Tremolati, M. Fanuli, B. Bassani, G. Farronato, A. Bruno, L. Mortara, *J. Immunol. Res.* **2018**, 2018, 8917804.
- [33] M. L. Sobah, C. Liongue, A. C. Ward, *Front. Med.* **2021**, 8, 727987.

- [34] E. J. Kucharz, M. Stajszczyk, A. Kotulska-Kucharz, B. Batko, M. Brzosko, S. Jeka, P. Leszczynski, M. Majdan, M. Olesinska, W. Samborski, P. Wiland, *Reumatologia* **2018**, 56, 203.
- [35] C. E. Egwuagu, J. Larkin III, *JAK-STAT* **2013**, 2, e24134.
- [36] M. Rath, I. Müller, P. Kropf, E. I. Closs, M. Munder, *Front. Immunol.* **2014**, 5, 5.
- [37] K.-D. Kröncke, K. Fehsel, V. Kolb-Bachofen, *Clin. Exp. Immunol.* **1998**, 113, 147.
- [38] P. Schilrreff, U. Alexiev, *Int. J. Mol. Sci.* **2022**, 23, 4928.
- [39] S. R. Thom, V. M. Bhopale, T. N. Milovanova, M. Yang, M. Bogush, D. G. Buerk, *J. Biol. Chem.* **2013**, 288, 4810.
- [40] E. Liu, *EMBO J.* **2003**, 22, 5036.
- [41] D. Lakens, *Front. Psychol.* **2013**, 4, 863.
- [42] S. Galarza, H. Kim, N. Atay, S. R. Peyton, J. M. Munson, *Bioeng. Transl. Med.* **2020**, 5, e10148.
- [43] R. Lv, Q. i Bao, Y. Li, *Mol. Med. Rep.* **2017**, 16, 9111.
- [44] M. J. Davis, T. M. Tsang, Y. Qiu, J. K. Dayrit, J. B. Freij, G. B. Huffnagle, M. A. Olszewski, *mBio* **2013**, 4.
- [45] F. Meng, C. A. Lowell, *J. Exp. Med.* **1997**, 185, 1661.
- [46] C. M. Ahmed, A. P. Patel, C. J. Ildefonso, H. M. Johnson, A. S. Lewin, *Transl. Vis. Sci. Technol.* **2021**, 10, 25.
- [47] A. R. Piñeros Alvarez, N. Glosson-Byers, S. Brandt, S. Wang, H. Wong, S. Sturgeon, B. P. McCarthy, P. R. Territo, J. C. Alves-Filho, C. H. Serezani, *JCI Insight* **2017**, 2, 92530.
- [48] H. M. Wilson, *Front. Immunol.* **2014**, 5, 357.
- [49] M. E. Long, W. E. Eddy, K.-Q. Gong, L. L. Lovelace-Macon, R. S. McMahan, J. Charron, W. C. Liles, A. M. Manicone, *J. Immunol.* **2017**, 198, 862.
- [50] S. Bournazos, T. T. Wang, J. V. Ravetch, *Microbiol. Spectr.* **2016**, 4.
- [51] E. Mendoza-Coronel, E. Ortega, *Front. Immunol.* **2017**, 8, 303.
- [52] J. Ma, K. Wei, J. Liu, K. Tang, H. Zhang, L. Zhu, J. Chen, F. Li, P. Xu, J. Chen, J. Liu, H. Fang, L. Tang, D. Wang, L. Zeng, W. Sun, J. Xie, Y. Liu, B. Huang, *Nat. Commun.* **2020**, 11, 11.
- [53] R. Chen, D. Yang, L. Shen, J. Fang, R. Khan, D. Liu, *Immun., Inflammation Dis.* **2022**, 10, e740.
- [54] W. Li, Y. Li, X. Jin, Q. Liao, Z. Chen, H. Peng, Y. Zhou, *Front. Oncol.* **2022**, 12, 775649.
- [55] C. S. Lim, D. W. Porter, M. S. Orandle, B. J. Green, M. A. Barnes, T. L. Croston, M. G. Wolfarth, L. A. Battelli, M. E. Andrew, D. H. Beezhold, P. D. Siegel, Q. Ma, *Front. Immunol.* **2020**, 11, 1186.
- [56] A. Egesten, M. Eliasson, A. I. Olin, J. S. Erjefält, A. Bjartell, P. Sangfelt, M. Carlson, *Int. J. Colorectal Dis.* **2007**, 22, 1421.
- [57] R. Günthner, H.-J. Anders, *Mediators Inflammation* **2013**, 2013, 731023.
- [58] K. Honma, H. Uono, T. Kohno, K. Yamamoto, A. Ogawa, T. Takemori, A. Kumatori, S. Suzuki, T. Matsuyama, K. Yui, *Proc. Natl. Acad. Sci. U. S. A.* **2005**, 102, 16001.
- [59] C.-F. Yu, W.-M. Peng, M. Schlee, W. Barchet, A. M. Eis-Hübing, W. Kolanus, M. Geyer, S. Schmitt, F. Steinhagen, J. Oldenburg, N. Novak, *J. Immunol.* **2018**, 200, 4024.
- [60] F. Seif, M. Khoshmirsafa, H. Aazami, M. Mohsenzadegan, G. Sedighi, M. Bahar, *Cell Commun. Signaling* **2017**, 151, 15.
- [61] M. A. Hoeksema, B. P. Scicluna, M. C. S. Boshuizen, S. Van Der Velden, A. E. Neele, J. Van Den Bossche, H. L. Matlung, T. K. Van Den Berg, P. Goossens, M. P. J. De Winther, *J. Immunol.* **2015**, 194, 3909.
- [62] D. Tweedie, W. Luo, R. G. Short, A. Brossi, H. W. Holloway, Y. Li, Q.-S. Yu, N. H. Greig, *J. Neurosci. Methods* **2009**, 183, 182.
- [63] Y. Nakano, T. Kasahara, N. Mukaida, Y. C. Ko, M. Nakano, K. Matsushima, *Infect. Immun.* **1994**, 62, 377.
- [64] N. Lotfi, R. Thome, N. Rezaei, G.-X. Zhang, A. Rezaei, A. Rostami, N. Esmaeil, *Front. Immunol.* **2019**, 10, 1265.
- [65] Y. Shi, C. H. Liu, A. I. Roberts, J. Das, G. Xu, G. Ren, Y. Zhang, L. Zhang, Z. R. Yuan, H. S. W. Tan, G. Das, S. Devadas, *Cell Res.* **2006**, 162, 126.
- [66] J. L. West, J. A. Hubbell, *Macromolecules* **1999**, 32, 241.
- [67] A. B. Kutikov, J. Song, *ACS Biomater. Sci. Eng.* **2015**, 1, 463.
- [68] J. Zhu, *Biomaterials* **2010**, 31, 4639.
- [69] T. T. Hoang Thi, E. H. Pilkington, D. H. Nguyen, J. S. Lee, K. i D. Park, N. P. Truong, *Polymers (Basel)* **2020**, 12, 298.
- [70] C.-C. Lin, K. S. Anseth, *Pharm. Res.* **2008**, 263, 631.
- [71] G. M. Cruise, D. S. Scharp, J. A. Hubbell, *Biomaterials* **1998**, 19, 1287.
- [72] X. Li, Q. Sun, Q. Li, N. Kawazoe, G. Chen, *Front. Chem.* **2018**, 6.
- [73] H. Liao, D. Munoz-Pinto, X. Qu, Y. Hou, M. A. Grunlan, M. S. Hahn, *Acta Biomater.* **2008**, 4, 1161.
- [74] M. B. Browning, T. Wilems, M. Hahn, E. Cosgriff-Hernandez, *J. Biomed. Mater. Res. Part A* **2011**, 98A, 268.
- [75] Q. T. Nguyen, Y. Hwang, A. C. Chen, S. Varghese, R. L. Sah, *Biomaterials* **2012**, 33, 6682.
- [76] M. E. Linder, R. J. Deschenes, *Nat. Rev. Mol. Cell Biol.* **2007**, 81, 74.
- [77] S. M. McCormick, N. M. Heller, *Front. Immunol.* **2015**, 6, 549.
- [78] P. Matricardi, C. Di Meo, T. Coviello, W. E. Hennink, F. Alhaique, *Adv. Drug Delivery Rev.* **2013**, 65, 1172.
- [79] D. L. Hern, J. A. Hubbell, *J. Biomed. Mater. Res.* **1998**, 39, 266.